Relating observed surface and subducted Subantarctic Mode Water in temperature-salinity space

R. Justin Small[1], Daniel B. Whitt[2], Ivana Cerovečki[3], Matthew Mazloff[3]

[1] National Center for Atmospheric Research, Boulder, CO, [2] Ames Research Center, National Aeronautics and Space Administration, Moffett Field, CA, [3] Scripps Institution of Oceanography, University of California San Diego, San Diego, CA

Supported by an award from the NASA Salinity Science program.

Introduction

The formation, subduction, and circulation of subantarctic mode water (SAMW) is crucial to the the nutrient, salinity, heat and carbon content in the global thermocline as well as air-sea exchange in a changing climate (Sarmiento et al. 2004, Frolicher et al. 2015, Terhaar et al. 2021). A conceptual model of SAMW dynamics has existed for decades, but it has proven difficult to simulate SAMW numerically and it has only recently become possible to observe SAMW variability with satellites and Argo.

We report preliminary results of a study that investigates the role of salinity and salinity circulation in SAMW dynamics (Small et al. 2021) and quantifies volume and properties of SAMW in temperature and salinity space.

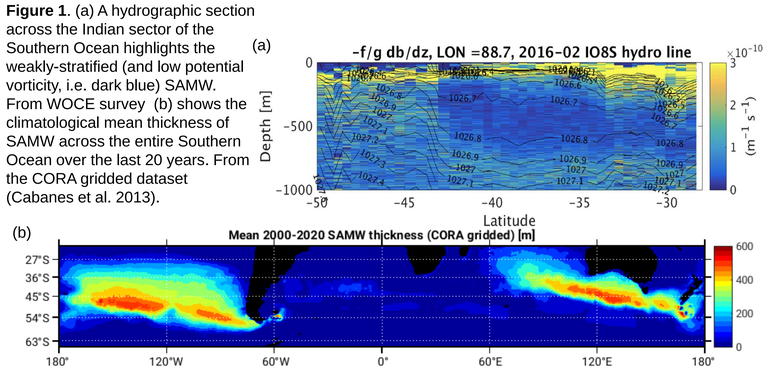

Figure 1. (a) A hydrographic section across the Indian sector of the Southern Ocean highlights the weakly-stratified (and low potential vorticity, i.e. dark blue) SAMW. From WOCE survey (b) shows the climatological mean thickness of SAMW across the entire Southern Ocean over the last 20 years. From the CORA gridded dataset (Cabanes et al. 2013).

Quantifying spatially and seasonally resolved differences between SSS from Aquarius and Argo.

One of the challenges in using satellite sea-surface salinity (SSS) to study SAMW formation and variability is that uncertainties remain about whether the satellite measurements are sufficiently accurate to allow this mid-to-high-latitude analysis of SSS anomalies. To address this question, we evaluate the accuracy of climatological variability represented by the satellite SSS by comparing it with near-surface observations from in-situ Argo floats. Specifically, we used the objectively analyzed and gridded SSS from Argo (Cabanes et al. 2013, "Argo" hereafter) and interpolate it to the objectively analyzed and gridded Aquarius SSS (OISSS: Melnichenko et al. 2016). We calculate the monthly climatology by averaging all years (2011-2014). The results indicate that there is significant (albeit small) seasonal high bias in the Aquarius OISSS that manifests mainly in Austral spring (e.g. October, Fig. 2). To correct for this, the climatological weekly bias is subtracted from the OISSS of Melnichenko et al. (2016) in order to obtain an OISSS product with negligible climatological bias (relative to Argo) that resolves mesoscale variability.

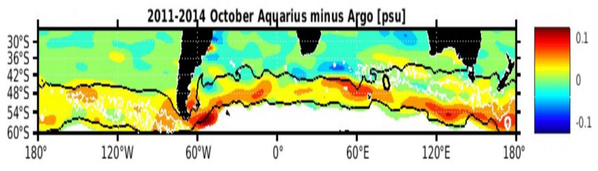

Figure 2. Climatological difference between OISSS from Aquarius (Melnichenko et al. 2016) and the OISSS from in-situ Argo profiles in October (2011-2014 only; Cabanes et al. 2013). High (yellow and red values) indicate satellite SSS is higher than Argo, whereas low (blue) indicate satellite SSS is lower than Argo. Black contours are the 26.6 and 27.1 kg/m³ density anomaly contours in the September 2000-2019 Argo climatology from Cabanes et al. (2013). The white contour is where the climatological September mixed layer depth is 300 m, as defined by the 0.03 kg/m³ density threshold method in the Holte et al. (2017) dataset.

Summary and Conclusions

Argo data, satellite salinity and a high-resolution climate model have been used to study SAMW formation.

Subducted SAMW occupies a narrow subset of the T-S between the SAMW density bounds. (Fig. 3). This allows us to determine the SAMW outcrop window from surface T and S alone, as opposed to previous assumptions that potential vorticity is also needed to determine SAMW outcrops.

The surface area with T-S of subducted SAMW approximately coincides with where mixed layers are deep and subduction occurs.(Fig. 4)

Satellite salinity and temperature data shows outcrop areas that are in qualitative agreement with that from Argo near-surface T/S.(Fig. 4) Quantitative differences may arise from differences in the data sampling and smoothing (Fig. 2) .

The high-resolution climate model reveals a narrow band of WMF in T/S space and in geographical space (Fig. 5) that coincides with the SAMW properties and location.

Future work: analysis of advection of salinity and stratification anomalies in SAMW: salinity and volume budgets in ECCO (ECCO consortium 2021a,b) and high-resolution CESM.

Surface and subducted SAMW volume in T-S space

Here SAMW is defined by potential density 1026.6 to 1027.1 kgm^{-3} and Potential Vorticity less than $40\times10^{-12}\ m^{-1}s^{-1}$, which is equivalent to very weak stratification. Monthly temperature (T) and salinity (S) are from the CORA ½◦ gridding of Cabanes et al. (2013). Here, we use 2000-2020, south of 20◦S.

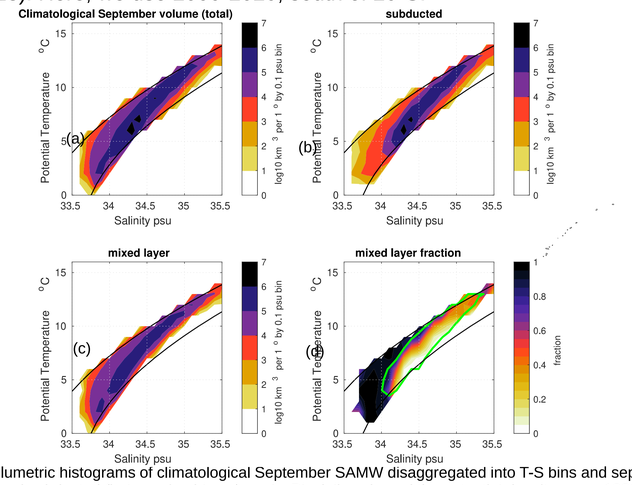

Figure 3. Volumetric histograms of climatological September SAMW disaggregated into T-S bins and separated into mixed-layer and subducted (below-mixed-layer) pools. Black lines bound the potential density range 1026.6-1027.1 kg/m³. (a) is the total volume, (b) is the subducted volume, (c) is the volume in the mixed layer, and (d) is the ratio mixed-layer over subducted volume. The green contour in (d) indicates subducted volume < 10^4 km³ per 1 deg/0.1 psu bin. Overlaid in (d) are the T/S properties of deep mixed layers identified by McCartney 1977 (his Fig 7) as examples of SAMW formation (small black circles).

Mixed-layer SAMW is spread more evenly across T/S space than subducted SAMW and dominates the freshest flavors <34.25 psu. Subducted SAMW occupies a narrow band in T/S space, <0.5 psu wide and <3ºC thick from 34.25 psu, 5ºC to 35.25 psu, 12ºC.

Outcrop areas on climatological timescales from bias-corrected satellite (--) and CORA gridded Argo (-)

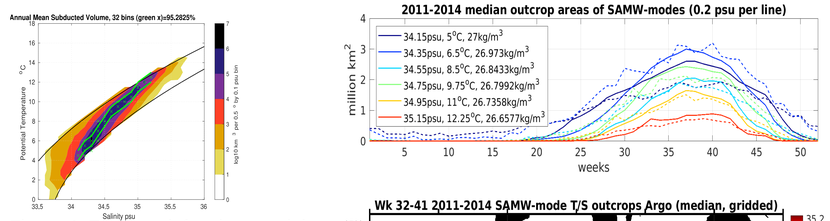

Figure 4. From top left to bottom right:

- Volume of annual-mean SAMW in T/S space. Green x indicate the bins included in the SAMW mode.
- Median over 2011-2014 weekly outcrop areas of the T/S classes from the SAMW mode (bias-corrected satellite (--) and gridded Argo (-)).
- Maps of median T/S class over week 32-41 and 2011-2014. Data are omitted (blank) if there is no T/S bin from the SAMW mode in any of the ten weeks in at least one of the 4 years.

Watermass formation by heat and freshwater fluxes

As part of this project we are using the high-resolution Community Earth System Model (CESM-HR, Small et al. 2014) to look at formation and advection of SAMW and how it relates to salinity.

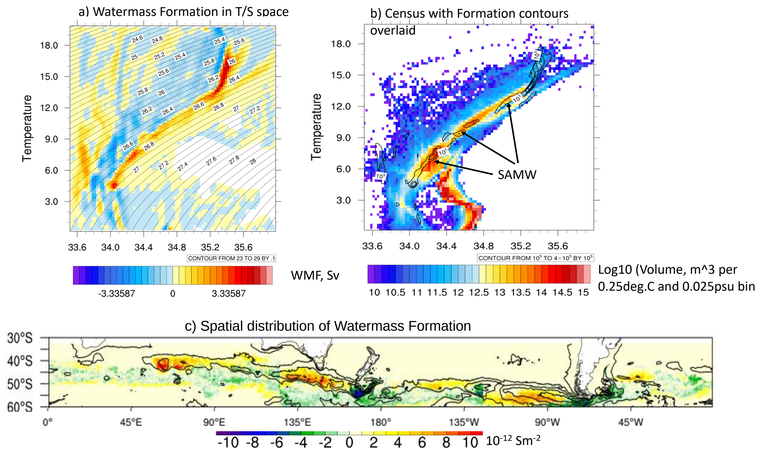

Figure 5. Upper panels: Surface watermass formation (WMF) in T/S space (left, Sv=10^6m^{3}s^{-1}) and volume census for low PV water, subducted (right). On the left panel potential density contours are overlaid. On the right panel the WMF contours are overlaid. Lower panel: Surface Water Mass Formation maps for 3 ocean sectors combined into one: WMF for PD between 1026.4 kgm^{-3} and 1026.6 kgm^{-3} for 0°-125° E, between 1026.6 kgm^{-3} and 1026.8 kgm^{-3} for 125° E to 125° W, and between 1026.8 kgm^{-3} and 1027 kgm^{-3} for 125° W to 0°. This method of combining different sectors allows for choice of the appropriate SAMW densities for each basin. Overlaid is the July-August –September average mixed layer depth from Argo (Whitt et al. 2019, JGR(O)), contours at 100m, 200m, 300m, 400m, 500m.

Above: Watermass Formation (WMF) has been computed in T/S space (Fig. 5a, Speer and Tziperman 1992). Note that formation (positive values) coincides with the SAMW branch of the census seen in Fig. 5b. Fig. 5c shows a watermass formation map (Maze et al. 2009): note that formation (positive values) occurs where the winter mixed-layer depth (contours) is deep in the SubAntarctic (see contours in Fig. 5c and also Fig. 1).

Acknowledgements and References – see next page

Relating observed surface and subducted Subantarctic Mode Water in temperature-salinity space

R. Justin Small[1], Daniel B. Whitt[2], Ivana Cerovečki[3], Matthew Mazloff[3]

[1] National Center for Atmospheric Research, Boulder, CO, [2] Ames Research Center, National Aeronautics and Space Administration, Moffett Field, CA, [3] Scripps Institution of Oceanography, University of California San Diego, San Diego, CA

Acknowledgements

NASA OSST project 19-OSST19-0012 “The Role of Salinity in the Subantarctic Mode Water Formation and Variability”. Optimally interpolated satellite salinity from Melnichenko et al. (2016). WOCE data was collected from a cruise in February 2016, on R/V Roger Revelle, chief scientist Allison Macdonald. Data gathered from https://cchdo.ucsd.edu/cruise/33RR20160208. CORA hydrographic data (Carbanes et al. 2013). CESM data (Small et al. 2014).

References

Argo (2021). Argo float data and metadata from Global Data Assembly Centre (Argo GDAC). SEANOE. http://doi.org/10.17882/42182

Cabanes, C., Grouazel, A., von Schuckmann, K., Hamon, M., Turpin, V., Coatanoan, C., Paris, F., Guinehut, S., Boone, C., Ferry, N. and de Boyer Montégut, C., 2013. The CORA dataset: validation and diagnostics of in-situ ocean temperature and salinity measurements. *Ocean Science*, *9*(1), pp.1-18.

ECCO Consortium, Fukumori, I., Wang, O., Fenty, I., Forget, G., Heimbach, P., & Ponte, R. M. 2021a. ECCO Central Estimate (Version 4 Release 4). Retrieved from URL ACCESSED December 2021.*

ECCO Consortium, Fukumori, I., Wang, O., Fenty, I., Forget, G., Heimbach, P., & Ponte, R. M. (2021b). Synopsis of the ECCO Central Production Global Ocean and Sea-Ice State Estimate (Version 4 Release 4). https://doi.org/10.5281/zenodo.4533349

Frölicher, T.L., Sarmiento, J.L., Paynter, D.J., Dunne, J.P., Krasting, J.P. and Winton, M., 2015. Dominance of the Southern Ocean in anthropogenic carbon and heat uptake in CMIP5 models. *Journal of Climate*, *28*(2), pp.862-886

McCartney, M., Subantarctic Mode Water, in A Voyage of Discovery (Suppl.to DeepSeaRes.),edited by M. Angel, pp. 103-119,Pergamon, New York, 1977.

Maze, G., G. Forget, M. Buckley, J. Marshall and I. Cerovecki, 2009. Using Transformation and Formation Maps to Study the Role of Air–Sea Heat Fluxes in North Atlantic Eighteen Degree Water Formation. J. Phys. Oceanogr., 39, 1818-1835.

Melnichenko, O., Hacker, P., Maximenko, N., Lagerloef, G. and Potemra, J., 2016. Optimum interpolation analysis of Aquarius sea surface salinity. Journal of Geophysical Research: Oceans, 121(1), pp.602-616

Sarmiento, J.L., Gruber, N., Brzezinski, M.A. and Dunne, J.P., 2004. High-latitude controls of thermocline nutrients and low latitude biological productivity. *Nature*, *427*(6969), pp.56-60.

Small, R.J. and co-authors (2014) A new synoptic scale resolving global climate simulation using the Community Earth System Model. J. Adv. Model. Earth Sys., 6, 1065-1094.

Small, R.J., DuVivier, A.K., Whitt, D.B., Long, M.C., Grooms, I. and Large, W.G., 2021. On the control of subantarctic stratification by the ocean circulation. *Climate Dynamics*, *56*(1), pp.299-327

Speer, K. and Tziperman, E., 1992. Rates of water mass formation in the North Atlantic Ocean. *Journal of Physical Oceanography*, *22*(1), pp.93-104

Sallée, J.B., Speer, K., Rintoul, S. and Wijffels, S., 2010. Southern Ocean thermocline ventilation. *Journal of Physical Oceanography*, *40*(3), pp.509-529

Terhaar, J., Frölicher, T.L. and Joos, F., 2021. Southern Ocean anthropogenic carbon sink constrained by sea surface salinity. *Science Advances*, *7*(18), p.eabd5964